Phospholipase A_2 Engineering. Probing the Structural and Functional Roles of N-Terminal Residues with Site-Directed Mutagenesis, X-ray, and NMR†

Xiaohong Liu,‡ Hongxin Zhu,‡ Baohua Huang,‡ Joseph Rogers,§ Bao-Zhu Yu,§ Amarendra Kumar,‡,|| Mahendra K. Jain,*,§ Muttaiya Sundaralingam,*,‡,|| and Ming-Daw Tsai*,‡,||

Departments of Chemistry and Biochemistry and The Ohio State Biochemistry Program, The Ohio State University, Columbus, Ohio 43210, and Department of Chemistry and Biochemistry, University of Delaware, Newark, Delaware 19716

Received November 10, 1994; Revised Manuscript Received March 20, 1995®

ABSTRACT: The N-terminal residues of phospholipase A_2 (PLA2) are believed to be involved in the hydrogen-bonding network, the interfacial binding site, or the hydrophobic channel. Site-directed mutants of bovine pancreatic PLA2 with substitutions at positions 2, 3, 4, 5, 6, and 9 were constructed to test the roles of these residues in the structure and function of PLA2. Nonconservative mutations of Phe-5 and Ile-9, which are located inside the hydrophobic channel, led to significant perturbations in the conformation and conformational stability. Kinetic studies also indicated that mutations at Ile-9 and Phe-5 caused significant decreases in the rate of hydrolysis toward micellar and vesicle substrates. Scooting mode kinetic analysis showed that the binding step of the mutant enzymes to the $DC_{14}PM$ (1,2-dimyristoyl-*sn*-glycero-3-phosphomethanol) vesicle interface is not significantly affected and that the perturbations in catalysis occur mainly in k_{cat} at the interface. The results taken together suggest that the residues Ile-9 and Phe-5 are important for both structure and catalysis. The mutant W3A (Trp-3 to Ala) also showed decreased rates of hydrolysis but to a lesser extent than Ile-9 and Phe-5 mutants. In addition, the binding affinity of W3A to the surface of the vesicles (i.e., the E to E* step) has been perturbed to the extent that hopping between anionic vesicles has been observed. On the other hand, the mutants of Gln-4 and Asn-6, which are located at or near the surface, displayed structural and kinetic properties similar to those of the wild-type PLA2 with the exception of the highly hydrophilic lysine mutant. The X-ray structure of the Q4E mutant indicates that the overall structure, the catalytic triad, and the link between residue 4 and Asp-99 via hydrogen bonding through Ala-1 and the structural water remain the same as in the WT. Substitutions for Leu at position 2 showed an acyl chain length discrimination toward different substrates, which may reflect the contacting position(s) of the substrate acyl chain with Leu-2.

The important structural elements for the catalytic reaction of phospholipase A_2 (PLA2)[1] include the catalytic diad (Asp-99••His-48), the calcium binding site (Asp-49 and three backbone carbonyl oxygens) (Dijkstra et al., 1981a,b; Scott et al., 1990), the hydrogen-bonding network (Dijkstra et al., 1981a) (Figure 1), the interfacial binding site (Dijkstra et al., 1981b, 1984; Scott et al., 1990; Ramirez & Jain, 1991), and the hydrophobic channel (Scott et al., 1990). The catalytic diad and the calcium binding site are obvious catalytic machinery for enzymes. The H-bonding network is thought to be important for catalysis by PLA2 since it connects the catalytic site to the interfacial binding site. The interfacial binding site is a functionally unique feature of

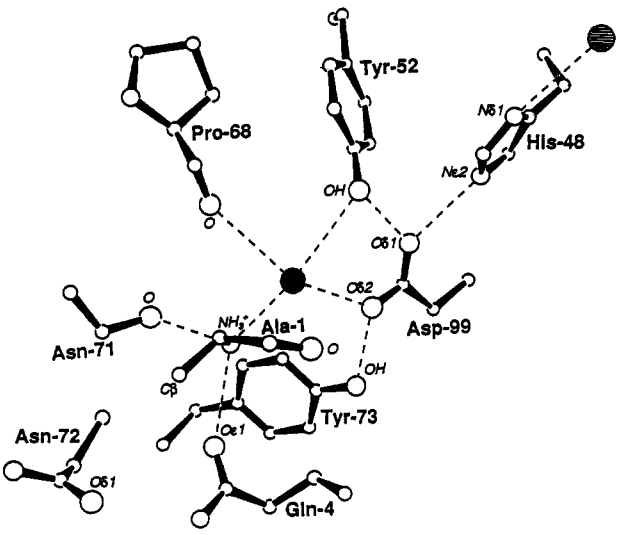

FIGURE 1: Schematic drawing of the H-bonding network in the crystal structure of PLA2. Reconstructed according to Dijkstra et al. (1983). The filled circle and the striped circle are structural water and catalytic water, respectively.

† The first three authors were responsible for approximately the same number of mutants. This work was supported by Research Grants GM41788 (to M.-D.T.), GM49547 (to M.S.), and GM29703 (to M.K.J.) from the National Institutes of Health. The Bruker AM-500 NMR spectrometer used was funded by NIH Grant RR01458. This is paper 15 in the series "Phospholipase A_2 Engineering" [for paper 14, see Tzeng et al. (1995)] and paper 4 in the series "Crystallography of Phospholipase A_2" [for paper 3, see Kumar et al. (1994)].

‡ The Ohio State Biochemistry Program.

§ University of Delaware.

|| Departments of Chemistry and Biochemistry, The Ohio State University.

® Abstract published in *Advance ACS Abstracts,* May 15, 1995.

[1] Abbreviations: CD, circular dichroism; COSY, correlated spectroscopy; 1D, one dimensional; 2D, two dimensional; DC_8PC, 1,2-dioctanoyl-*sn*-glycero-3-phosphocholine; DC_8PM, 1,2-dioctanoyl-*sn*-glycero-3-phosphomethanol; $DC_{14}PM$, 1,2-dimyristoyl-*sn*-glycero-3-phosphomethanol; DTPM, 1,2-ditetradecyl-*sn*-glycero-3-phosphomethanol; EDTA, ethylenediaminetetraacetate; FPLC, fast protein liquid chromatography; GB, Gaussian broadening; Gdn·Cl, guanidine hydrochloride; LB, line broadening; MJ33, 1-hexadecyl-3-(trifluoroethyl)-*rac*-glycero-2-phosphomethanol; NOE, nuclear Overhauser effect; NOESY, nuclear Overhauser enhancement spectroscopy; pH*, pH in D_2O without correction for the deuterium isotope effect; PLA2, phospholipase A_2; TMSP, sodium 3-(trimethylsilyl)[2,2,3,3-$^2H_4$]propionate; WT, wild type.

0006-2960/95/0434-7322$09.00/0

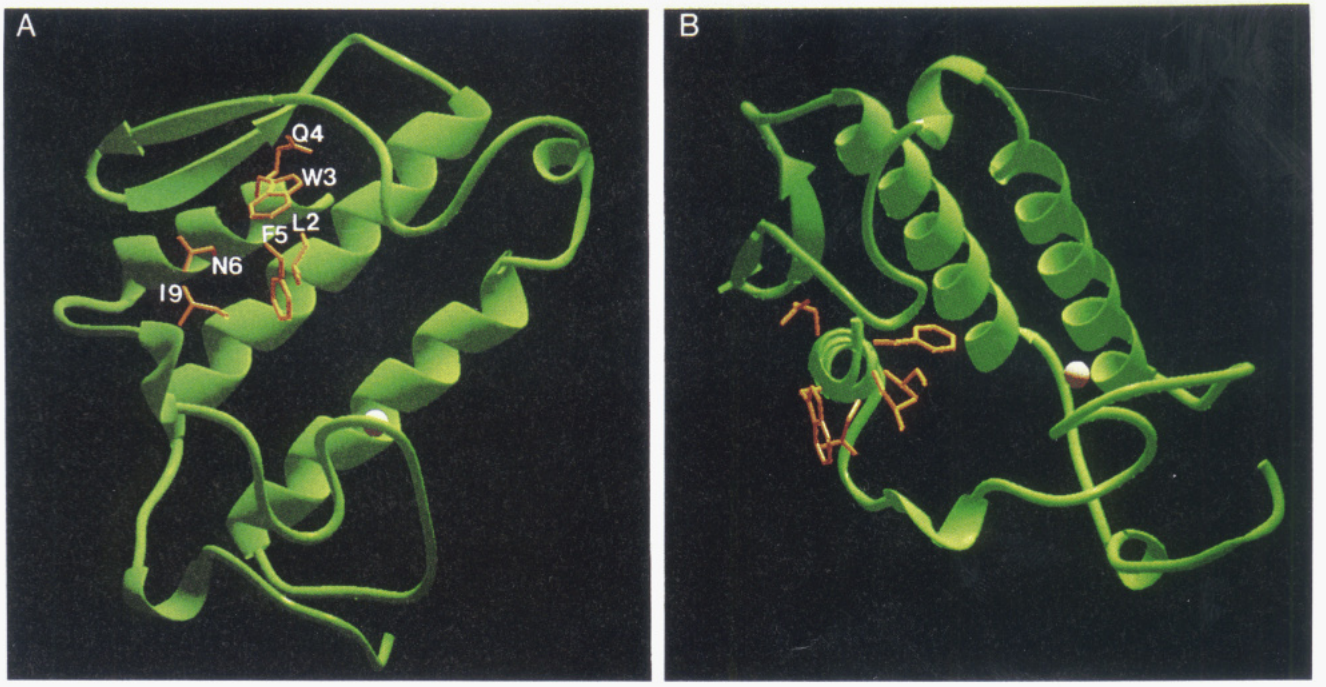

FIGURE 2: Ribbon diagrams (Carson, 1991) of PLA2 showing the disposition of the side chains of Leu-2, Trp-3, Gln-4, Phe-5, Asn-6, and Ile-9 of the N-terminal helix as well as the calcium ion (gray sphere). In view A, the N-terminal helix axis is nearly along the plane of the figure, while in view B, it is approximately perpendicular.

PLA2 (Dijkstra et al., 1981a,b; Ramirez & Jain, 1991) since it has been established that the binding of PLA2 to the substrate interface must precede the catalytic turnover at the interface (Jain & Berg, 1989) and that binding of the enzyme to the interface increases its affinity for the active site-directed ligands (Jain et al., 1993). The hydrophobic channel is thought to allow passage of a substrate molecule from the substrate surface to the active site (Scott et al., 1990). These structural elements have been identified mainly by physical methods, and their functional significance needs to be established by kinetic studies.

Having developed the ability to analytically dissect the primary kinetic and equilibrium parameters for interfacial catalysis (Berg et al., 1991; Yu et al., 1993; Jain et al., 1995), we have used site-directed mutagenesis coupled with NMR, X-ray, and kinetic analyses to critically evaluate the structural and functional roles of the catalytic diad (Dupureur et al., 1990; Li & Tsai, 1993), the calcium binding site (Li et al., 1994), and part of the H-bonding network (Dupureur et al., 1992a,c; Sekharudu et al., 1992; Kumar et al., 1994) in bovine pancreatic PLA2. Our system is bovine pancreatic PLA2 overexpressed in *Escherichia coli* (Deng et al., 1990). Several unexpected significant results have been found: the catalytic diad is important not only for catalysis but also for maintaining the structural integrity of the enzyme (Li & Tsai, 1993); deletion of part of the hydrogen bonds in the hydrogen-bonding network has minimal effect on the catalytic activity (Dupureur et al., 1992a,c) or structure (Sekharudu et al., 1992); the D99N mutant which loses its structural water in the H-bonding network (Kumar et al., 1994) and the deletion mutant without Ala-1 which is critical for holding the structural water (Maliwal et al., 1994) still retain significant catalytic activity.

We now turn our attention to the N-terminal region, which is intimately involved in the H-bonding network, the interfacial binding site, and the hydrophobic channel. The importance of Ala-1, a residue at the interfacial recognition region (Dijkstra et al., 1981a, 1983), in the binding of the substrate to the active site has already been reported recently (Maliwal et al., 1994). The structural and functional significance of six other N-terminal residues is developed in this work: Gln-4, which is part of the H-bonding network as shown in Figure 1, Trp-3 and Asn-6, which are part of the interfacial binding site (Dijkstra et al., 1981b, 1984; Scott et al., 1990), and Leu-2, Phe-5, and Ile-9, which are part of the hydrophobic channel (Scott et al., 1990). Figure 2 highlights the side chains of these residues. Gln-4 is conserved among all known sequences of PLA2, except that it is replaced by Glu or Asn; both are also capable of forming hydrogen bonds *via* side chains in a few cases (Davidson & Dennis, 1990; Heinrikson, 1991). Trp-3 is conserved among pancreatic PLA2s, but it is usually a different hydrophobic residue in other types of PLA2. The spectroscopic properties of Trp-3 have been used to show that the N-terminus is indeed perturbed upon interfacial binding (van Scharrenburg et al., 1982, 1984a,b; Ramirez & Jain, 1991). Position 6 is usually an arginine in pancreatic PLA2 from other animals (Davidson & Dennis, 1990; Heinrikson, 1991). Residues Ile-9 and Phe-5 are two absolutely invariant residues among all known (>50) PLA2 sequences except for a Leu variant for Phe-5 (van den Bergh et al., 1989; Davidson & Dennis, 1990). Leu-2 is also highly conserved, except that it is replaced by other hydrophobic residues, valine or phenylalanine in a few cases.

According to the crystal structure of the complex of snake venom PLA2 and a transition-state analog, L-1-*O*-octyl-2-(heptylphosphonyl)-*sn*-glycero-3-phosphoethanolamine (White et al., 1990; Scott et al., 1990), the side chains of the three hydrophobic channel residues (Leu-2, Phe-5, and Ile-9) could contribute to substrate binding by providing their hydrophobic surface to contact the acyl chain of the substrate. The X-ray crystal structure of porcine pancreatic PLA2 complexed with another inhibitor, 2-(dodecanoylamino)-1-hexanol phosphoglycol, also shows that Ile-9 is located close to the *sn*-2 acyl chain, with its δ-methyl group located only 3.60 Å away from the C9 position of the *sn*-2 acyl chain of

the inhibitor (Thunnissen et al., 1990). Evidence of direct interaction between Ile-9 and Phe-5 side chains and the transition-state analogs has also been provided by the inhibitor−protein NOEs of porcine pancreatic PLA2 bound to a micellar lipid−water interface of different substrate-derived competitive inhibitors (Dekker et al., 1991; Peters et al., 1992). In their studies, large chemical shift changes for Ile-9 and Phe-5 were observed when the inhibitors bound in the active site. The δ-methyl group of Ile-9 was clearly shown to interact at position C9 or C10 of the competitive inhibitors, while a strong intermolecular NOE from the aromatic protons of Phe-5 was clearly assigned to one of the methylene protons of the *sn*-2 chain of the inhibitor. The NMR analyses, however, did not identify direct contact between the Leu-2 side chain and the inhibitor.

In this study, the structural roles of the residues were examined by analyzing the conformational stability and the proton NMR properties of the mutants. The functional roles were analyzed by micellar and vesicle (scooting mode) kinetics. The results suggest the following: (i) The specific structural and functional roles for Gln-4 and Asn-6 are minimal. The crystal structure of Q4E also indicates overall similarity with that of WT, except the side-chain structure of residue 4. (ii) W3A shows modest perturbations in kinetic parameters and in the binding to the interface (the E to E* step). (iii) The hydrophobicity of the Phe-5 and Ile-9 side chains is essential for full catalytic activity in the chemical step. (iv) Nonconservative mutations of Phe-5 and Ile-9 led to significant perturbations in the conformation and conformational stability. (v) Substitutions for Leu at position 2 showed an acyl chain-length discrimination for the enzyme activity toward substrates DC_8PC, DC_8PM, or $DC_{14}PM$, which may reflect the contacting position(s) of the substrate acyl chain with Leu-2.

MATERIALS AND METHODS

Materials and Routine Procedures. Oligonucleotides were obtained from the Biochemical Instrument Center at The Ohio State University or The Midland Certifide Reagent Co. (Midland, TX). Mutagenesis and sequencing kits were purchased from Amersham and United States Biochemicals, respectively. All restriction enzymes and incubation buffers were obtained from GIBCO BRL. The following lipids were synthesized as described previously: DTPM (Jain et al., 1986); DC_8PM (Jain & Rogers, 1989); $DC_{14}PM$ (Jain & Gelb, 1991); MJ33 (Jain et al., 1991c). All other phospholipid substrates used in this study were purchased from Avanti Polar Lipids (Birmingham, AL). Ultrapure guanidine hydrochloride was purchased from ICN Biochemicals; 99.9 atom % D D_2O, "100% D" D_2O, and TMSP were obtained from MSD Isotopes. The Fast Flow Sepharose-S and -Q resins (cation and anion exchangers, respectively) used for FPLC columns were purchased from Pharmacia-LKB. Other chemicals and biochemicals were of the highest quality available commercially. FPLC experiments were performed on a Pharmacia-LKB FPLC system.

Construction and Purification of Mutant Enzymes. For Q4A, Q4E, Q4N, and Q4K, the mature PLA2 gene from the pTO-A2M plasmid (Deng et al., 1990) was used to construct the mutants; for all other mutants the pro-PLA2 gene from the pTO-propla2 plasmid (Deng et al., 1990) was used. Site-directed mutants were generated by using an Amersham mutagenesis kit according to the manual provided by the manufacturer. W3A was constructed from the oligonucleotide 5′GTTAAACTGCGCAAGAGCACG3′, where the underlined bases represent the mutated sites. The oligonucleotides used for the construction of Q4A, Q4E, Q4N, and Q4K were 5′CCGTTAAACGCCCAAAGAGC3′, 5′CCGTTAAACTCCCAAAGAGC3′, 5′CCGTTAAATTGCCAAAGAGC3′, and 5′CCGTTAAATTCCCAAAGAGC3′, respectively. The mutants N6A and N6D were obtained from a degenerate oligonucleotide 5′GATCATTCCG(G/T)CAAACTGCCA3′. All the mutants at position Ile-9 were obtained from two degenerate oligonucleotides: 5′ACATTTGA(A/C)CATTCCGT3′ for I9V/I9F and 5′ACATTTG(T/G)(C/A)CATTCCGT3′ for I9A, I9S, and I9Y. Both F5A and F5V mutants were obtained from a degenerate oligonucleotide: 5′CATTCCGTTA(A/G)CCTGCCAAAGAGCAC3′. The F5W mutant was constructed using oligonucleotide 5′GATCATTCCGTTGTACTGCCAAAGAGCACG3′, and the F5Y mutant was made from oligonucleotide 5′GACATTCCGTTCTACTGCCAAAGAGCACG3′. The double mutant F5V/I9F was constructed on the DNA template of the single mutant I9F, using the same oligonucleotide for F5V. The Leu-2 mutants were constructed from oligonucleotides in which the underlined bases in 5′AAACTGCCAAAGAGCACGAGA3′ were replaced by AGC, CCA, and CCT for L2A, L2W, and L2R, respectively.

The resulting mutants were verified by direct sequencing with the dideoxy-chain-termination method (Sanger et al., 1977). Recombinant PLA2 was isolated from the *E. coli* expression host, BL21(DE3) [pLysS], carrying the pTO-propla2 plasmid (pTO-A2M in the case of Q4 mutants) as described elsewhere (Noel et al., 1991; Dupureur et al., 1992a,b; Li & Tsai, 1993). The routine large-scale preparation of PLA2 was achieved by growth of 10 L of culture. The fusion proteins were activated by trypsin cleavage.

NMR Analysis. Ten milligrams of enzyme was dissolved in 0.5 mL of D_2O (99.9 atom % D) containing 300 mM NaCl and 50 mM $CaCl_2$, kept at room temperature for 4 h to allow for deuterium exchange, and then lyophilized. After the exchange step was repeated, the sample was dissolved in 0.5 mL of "100%" D_2O, and the pH* (uncorrected pH directly from pH meter reading) was adjusted to 4.0 by using DCl and NaOD stock solutions. Spectra were obtained on a Bruker AM-500 spectrometer at 37 °C. Sodium 3-(trimethylsilyl)[2,2,3,3-$^2H_4$]propionate (TMSP) was used as an internal chemical shift reference. Solvent suppression by presaturation was applied in all experiments. Typically 200 scans were collected for one-dimensional spectra. Gaussian multiplication (GB 0.1, LB −5.0) was applied to the frequency-induced decay prior to Fourier transformation. A 200 ms mixing time was applied for all two-dimensional NOESY experiments. A 4096 × 512 matrix in the time domain was recorded and zero-filled to a 4096 × 2048 matrix prior to multiplication by a Gaussian function (GB 0.1, LB −3.0).

Gdn·HCl-Induced Denaturation and Conformational Stability. CD spectra were recorded on a JASCO J-500C spectropolarimeter using a thermostated quartz microcell and processed using DP-500/AT system (version 1.29) software. A stock solution of ca. 8.5 M Gdn·HCl was prepared in a buffer containing 10 mM borate and 0.1 mM EDTA, pH 8.0, and the exact concentration was determined by refractive index (Nozaki, 1972). An enzyme solution of approximately 3 mg/mL was prepared in the same buffer, and the precise concentration was measured spectrophotometrically. Samples,

which contained 0.05 mg/mL enzyme, the borate buffer mentioned above, and various concentrations of Gdn·HCl, were incubated at 30 °C for 10 min and then scanned 5 times from 250 to 200 nm. The ellipticity at 222 nm was recorded and used to determine the free energy of unfolding, $\Delta G_d^{H_2O}$.

Kinetics Analysis. Activities toward micellar DC_8PC substrates were carried out at 45 °C, pH 8.0, on a Radiometer RTSS titration system as described previously (Noel et al., 1991). The assay mixtures consist of 100 mM NaCl, 25 mM $CaCl_2$, 1 mM sodium borate, 0.1 mM EDTA, and varying concentrations of DC_8PC. The apparent V_{max} and apparent K_m were determined from Eadie–Hofstee plots (Atkins & Nimmo, 1975) of v vs v/[S] through the use of linear regression analyses. On the basis of a molecular weight of 13 500, the $k_{cat,app}$ was calculated from the apparent V_{max}. The initial rate of hydrolysis of DC_8PM (at 0.115 mM) was monitored by pH-stat in the presence of 1 mM NaCl and 1 mM $CaCl_2$, pH 8, at 22 °C. Under this condition pancreatic PLA2 is known to form premicellar aggregates with this substrate (Jain & Rogers, 1989); however, the substrate does not precipitate or phase separate. The estimated errors for the kinetic data of micelles are within ±10%.

Kinetics analysis of PLA2 in the scooting mode on DC_{14}-PM vesicles was conducted as described previously using a pH-stat method under first-order (Jain et al., 1986; Jain & Gelb, 1991; Berg et al., 1991) or zero-order (Berg et al., 1991; Jain et al., 1991b) conditions. The turnover number at the maximal mole fraction of the substrate (v_0), the apparent second-order rate constant ($N_S k_i$), and the Michaelis constant at the interface (K_M*) were obtained by deconvolution of the reaction progress curve.

Dissociation Constants. The equilibrium dissociation constants for the dissociation of calcium (K_{Ca}*),[2] inhibitors (K_I*), products (K_P*), and substrate analogs (K_S*) bound to the active site of PLA2 at the interface were determined by monitoring the rate of alkylation of His-48 by *p*-nitrophenacyl bromide as described elsewhere (Jain et al., 1991a). The remaining PLA2 activity of each protection reaction in the presence of ligands was detected as a function of time. The value of K_M* was calculated by three independent methods: (a) from the integrated Michaelis–Menten equation to describe the whole reaction progress curve (Berg et al., 1991); (b) from a relationship between K_I* and the mole fraction of the inhibitor required for 50% inhibition (Jain et al., 1991a); (c) from K_{Ca}* and K_{Ca}*(S), the apparent dependence of v_0 on the calcium concentration (Yu et al., 1993). The uncertainty in these values is about ±15%.

X-ray Crystallography. Crystals of Q4E were grown by the hanging drop vapor diffusion method using the conditions described earlier (Noel et al., 1991). The crystals are orthorhombic and isomorphous to the wild-type PLA2 (Dijkstra et al., 1981a) with the space group $P2_12_12_1$ and cell dimensions a = 46.83 Å, b = 64.57 Å, and c = 38.57 Å.

[2] Definition of kinetic parameters *at the interface*: K_{Ca}*, dissociation constant for Ca^{2+} determined by the protection method; K_{Ca}*(S), effective dissociation constant for Ca^{2+} under catalytic conditions at a mole fraction of 1 of the substrate; K_I*, dissociation constant of inhibitor; K_M*, Michaelis constant; K_P*, dissociation constant of product; K_S*, dissociation constant of substrate; k_{cat}, turnover number at saturating substrate concentration; $N_S k_i$, apparent second-order rate constant; v_0, turnover number at X_S = 1; X_I, mole fraction of inhibitor. For complete analytical formalism and definitions, see Berg et al. (1991) and Jain et al. (1995).

Table 1: Summary of Kinetic Data for WT and Mutants[a]

	DC_8PC		$DC_{14}PM$	DC_8PM
enzyme	$K_{m,app}$ (mM)	$k_{cat,app}$ (s^{-1})	v_0 (s^{-1})[b]	v^b (s^{-1})
WT	1.4	680	330	750
L2A	2.0	700	100	770
L2W	0.9	650	10	540
L2R	2.7	1.5	0.014	6.3
W3A	7.7	96	80	520
Q4A	19	395	185	460
Q4E	3.7	670	220	860
Q4N	0.8	420	105	430
Q4K	*c*	60[c]	130	350
F5A	9.8	13	2	5
F5V	3.0	7.6	2	6.2
F5Y	2.3	45	3.6	27
F5W	1.5	3.4	3.3	5.8
N6A	2.3	600	320	430
N6D	6.9	1870	380	280
I9V	2.3	970		
I9A	9.3	20	50	130
I9S	8.7	49	22	150
I9F	2.3	12	20	60
I9Y	6.0	3.6	6.0	8.4
F5V/I9F		<0.1		

[a] The estimated errors are ±10%. [b] Initial rate of hydrolysis at 0.115 mM substrate concentration. [c] Calculated from the specific activity at 5 mM DC_8PC. The $K_{m,app}$ was not determined due to the low yield of this mutant.

Intensity data to 1.8 Å were collected, at room temperature, on our Siemens four-circle area detector as described earlier (Kumar et al., 1994). The crystal to detector distance was 12 cm. The data were obtained from a ϕ-scan (0–135°) and two ω-scans (3–310°) at χ = 45° and 90°. The exposure time used was 60 s per frame. The data were processed by XENGEN 2.0 (Howard, 1990). Of the 29 470 reflections, 10 302 were unique with an R_{sym} of 5.0%. The orthorhombic structure (Dijkstra et al., 1981a) with Glu-4 instead of Gln-4 was taken as the starting model and refined by the rigid body method (Brünger, 1992) using 1829 reflections ($F > 5$) in the resolution range 6.0–3.0 Å. This gave an R-value of 23%. Further refinement by simulated annealing reduced the R-value to 19.5%. The model was refitted using FRODO 6.6 (Jones, 1985) on our Evans and Sutherland molecular graphics system (ESV30). Refinement of positional and thermal B factors including water molecules located from difference electron density and omit $2F_o - F_c$ maps gave an R-value of 17.0% for 8065 reflections [$F > 2\sigma(F)$] in the resolution range 6.5–1.8 Å. The final model consists of 957 protein atoms, 1 calcium ion, and 78 water molecules.

RESULTS

Apparent Catalytic Constants toward DC_8PC Micelles. The apparent kinetic constants $k_{cat,app}$ and $K_{m,app}$ of all mutants toward DC_8PC micelles are listed in Table 1. The kinetic behavior of the mutants can be classified into three categories. (a) Little or no changes in $k_{cat,app}$ and $K_{m,app}$: These include the mutants of Leu-2 (with the exception of the highly hydrophilic mutant L2R) and Asn-6. (b) Modest decreases in $k_{cat,app}$ and/or modest increases in $K_{m,app}$: These include W3A (7-fold decrease in $k_{cat,app}$ and a 5-fold increase in $K_{m,app}$), Q4A (2-fold decrease in $k_{cat,app}$ and a 13-fold increase in $K_{m,app}$), and Q4K (50-fold decrease in specific activity). On the other hand, the $k_{cat,app}$ and $K_{m,app}$ of Q4E and Q4N are almost unchanged, possibly because the hydrogen bond between the side chain of residue 4 and the N-terminal ammonium group can be preserved in these two

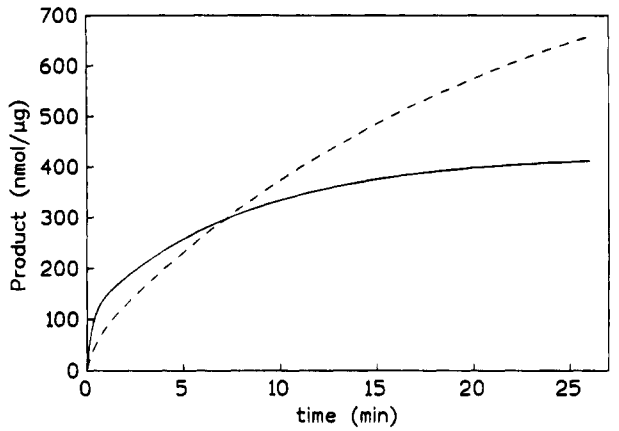

FIGURE 3: Reaction progress curves for the hydrolysis of $DC_{14}PM$ (0.3 mM) vesicles in 4 mL of 0.5 mM $CaCl_2$ and 1 mM NaCl, at 25 °C and pH 8.0. The reaction was initiated with addition of 0.35 mg or 25 pmol of the Q4A (solid line) or W3A (dashed line) mutant. The ordinate is expressed as nanomoles of products formed per microgram of enzyme.

conservative mutants. (c) Large perturbations with the mutants of Phe-5 and Ile-9: All four mutants of Phe-5 show decreased $k_{cat,app}$ (15−200-fold), and F5A shows a 7-fold higher $K_{m,app}$. For the residue Ile-9, all of the five mutants, except the most conservative mutation I9V, show decreased $k_{cat,app}$ (14−190-fold) and increased $K_{m,app}$ (up to 7-fold). Overall, the data for the Ile-9 and Phe-5 mutants indicate that $k_{cat,app}$ decreases upon removal of the hydrophobic bulk (I9A and F5A), increase of the hydrophobic bulk (I9F and F5W), or introduction of hydrophilicity (I9S, I9Y, and F5Y).

We have attempted to compensate for the losses of activity in F5V by making a double mutant I9F/F5V, hoping that the two hydrophobic mutations can make up for each other. Such a switch of hydrophobic side chain appears to be allowed on the basis of computer modeling. However, this mutant enzyme displays a greater decrease in $k_{cat,app}$ (<0.1 s^{-1}), as also shown in Table 1. No further kinetic analysis has been conducted for this double mutant.

Interfacial Catalysis and Binding of the Enzyme to the Interface. Since the kinetic constants for micelles are only apparent values representing a combination of interfacial binding and catalytic steps at the interface, we further performed detailed analyses using $DC_{14}PM$ vesicles to dissect these steps in terms of primary rates and equilibrium constants (Berg et al., 1991). Since the equilibrium constant for the binding of pancreatic PLA2 to the anionic surface is quite favorable, the contribution of the interfacial binding step to the overall catalytic turnover can be readily eliminated by monitoring the rate of hydrolysis at such an interface in the highly processive scooting mode.

The protocols for monitoring interfacial catalysis in the scooting mode (Jain et al., 1986, 1991c; Berg et al., 1991) were used to characterize the kinetic properties of the mutants. The reaction progress curves for the hydrolysis of $DC_{14}PM$ in the form of small sonicated vesicles were apparently first order (data not shown). In all cases, except W3A, the initial phase of activity ceased before all the substrate present in the reaction mixture was hydrolyzed. Since the reaction essentially stopped at the end of this phase, it suggested that the intervesicle exchange of enzyme is essentially negligible over the time course of the reaction. However, analysis of the whole reaction progress curves (Figure 3) indicated that the product obtained per unit of enzyme for W3A (dashed line) does not level off, in contrast to the curves of other mutants (Q4A as an example, solid line) and WT (Jain et al., 1991b). This suggests that the affinity of the enzyme to the anionic vesicle interface (i.e., the E to E* step) has decreased to the extent that some hopping has occurred for W3A. Similar hopping has also been induced from $DC_{14}PM$ vesicles by salt (Jain et al., 1991b) or by increasing the mole fraction of zwitterionic PC in the anionic $DC_{14}PM$ vesicles (Ghomashchi et al., 1991).

Table 2: Catalytic and Equilibrium Parameters for the Hydrolysis of $DC_{14}PM$ by WT and Mutants[a]

parameters	WT	L2A	W3A	Q4A	F5V	I9A
v_0 (s^{-1})	330	100	80	185	2	50
alkylation time (min)	<1	3.4	1.5	1.4	1.8	5
$X_I(50)$ MJ33	0.025	0.1	0.05	0.018	0.012	0.027
K_I* (MJ33)	0.01	0.01	0.04	0.011	0.003	0.0037
K_S* (DTPM)	0.02	0.023	0.06	0.06	0.005	0.032
K_P*	0.025	0.006	0.05	0.02	0.002	0.0053
K_{Ca} (mM)	0.5	1.1	0.4	0.29	1.1	2.2
K_{Ca*} (mM)	0.35	0.39	0.13	0.32	0.45	1
K_{Ca}*(S) (mM)	0.15	0.06	0.1	0.2	0.09	0.13
v_0/N_SK_i	11	10	15	30		12
K_M* from K_P* and RPC	0.4	0.06	2.5	1.4		0.07
K_M* from $X_I(50)$	0.65	0.1	3.3	1.5	0.33	0.16
K_M* from K_{Ca}*(S)	0.7	0.18	3.3	1.7	0.25	0.15
k_{cat} (s^{-1})	500	110	320	460	2.6	55

[a] The error limits are estimated to be ±15% for the values in this table.

The intrinsic rate of the catalytic turnover can be best seen in the values of v_0, the steady-state rate of hydrolysis of DC_{14}-PM vesicles at the mole fraction of substrate $X_S = 1$. As summarized in Table 1, all mutants with decreased $k_{cat,app}$ also show decreased v_0. The v_0 values for the Ile-9 mutants decrease by 7−55-fold, whereas those of the Phe-5 mutants decrease by 90−165 fold.

Activities toward DC_8PM Micelles. Qualitatively, the degree of changes in the v_0 of $DC_{14}PM$ vesicles is consistent with that in the $k_{cat,app}$ of DC_8PC micelles. This correlation has been observed in most of the mutants reported previously (Dupureur et al., 1992a,b; Li et al., 1994). However, the Leu-2 mutants display a significantly different trend: the decreases in v_0 are significantly greater than the decreases in $k_{cat,app}$. A possible origin for this difference is that, since Leu-2 is located at the entrance of the hydrophobic channel, its side chain affects substrates with long acyl chains but not short acyl chains. In order to substantiate this interpretation, we determined the initial rate of hydrolysis of DC_8-PM, which has the same headgroup as $DC_{14}PM$ but the same acyl chain as DC_8PC. The results, as listed in Table 1 (last column), indicate that the activities of Leu-2 mutants toward DC_8PM parallel those toward DC_8PC, which suggests that the acyl chain length rather than the headgroup is the main determinant.

Specific Steps of Perturbation at the Interface. The basis for the loss of catalytic activity was examined further by characterization of the kinetic and equilibrium binding parameters for one mutant at each position: L2A, W3A, Q4A, F5V, and I9A. The results are summarized in Table 2. The equilibrium dissociation constants at the interface for inhibitors (K_I*), the products of hydrolysis (K_P*), calcium (K_{Ca} and K_{Ca}*), and substrate analog DTPM (K_S*) were determined by monitoring the rate of alkylation of His-48 by *p*-nitrophenacyl bromide as described previously (Jain et

al., 1991a). Values of K_M* were calculated from initial rates of hydrolysis of $DC_{14}PM$ in the absence and presence of the competitive inhibitor MJ33 [$(v_0)^0$ and $(v_0)^I$, respectively] according to the equation (Berg et al., 1991; Jain et al., 1991a):

$$(v_0)^0/(v_0)^I = 1 + [(1 + 1/K_I^*)/(1 + 1/K_M^*)][X_I/(1 - X_I)]$$

where X_I is the mole fraction of the inhibitor and K_I* is the dissociation constant of the inhibitor. In addition, K_M* was also calculated from the relationship between K_{Ca}*(S) and K_{Ca}* values (Yu et al., 1993), as well as from K_P* and the reaction progress curve if the observed v_0 value was more than 50 s^{-1}.

The data in Table 2 indicate that the mutants of Phe-5 and Ile-9, which display the largest decreases in $k_{cat,app}$ and v_0, are most highly perturbed in the k_{cat} at the interface: I9A shows a 10-fold decrease, and F5V displays a 200-fold decrease in k_{cat}. Thus the perturbations in the kinetic properties of I9A and F5V occur mainly at the chemical step at the interface. In addition, I9A also shows 5-fold decreases in K_M* and K_P*, as well as a 5-fold increase in the alkylation time; F5V shows a 10-fold decrease in K_P*; W3A shows 6−8-fold increases in K_M*; L2A shows 5-fold decreases in K_M* and K_P*.

In summary, the results of both micellar and scooting mode kinetic analyses indicate that the mutants of Phe-5 and Ile-9, whose side chains point into the hydrophobic channel, are most highly perturbed. The other mutants are less perturbed possibly because they are located at or near the surface. Mutants of these residues were expected to perturb the E to E* step, but such a perturbation was observed on the anionic interface only for W3A.

Structural Properties. Although the main focus of this work is on interfacial catalysis, it is important to analyze the structures of the mutant enzymes for two reasons: First, perturbation of the hydrogen-bonding network could greatly perturb the conformational dynamics of PLA2, as has been demonstrated for D99N (Dupureur et al., 1992c) and H48N and H48A (Li & Tsai, 1993). Second, the structural information is important for the interpretation of kinetic data and the structure−function relationship. If the conformation of a mutant is unperturbed, the changes in kinetic constants can be used to explain the functional role of the mutated residue. On the other hand, if a large perturbation in conformation is observed, one cannot attribute the changes in kinetic constants solely to the functional role of the mutated residue. We therefore examined the structural perturbations of the mutant enzymes by comparing their conformational stability and proton NMR properties with those of WT PLA2.

Conformational Stability. The conformational stability of all mutants was measured by Gdn·HCl-induced denaturation, monitored by CD spectroscopy. Comparison of the CD spectra (200−250 nm) for WT and all mutants showed only minor differences and suggested that the secondary structures are largely preserved. The denaturation curves display a behavior consistent with an apparent two-state folding mechanism (data not shown). The denaturation data were analyzed by the equation (Pace, 1986):

$$\Delta G_d = \Delta G_d^{H_2O} - m[\text{Gdn·HCl}]$$

where ΔG_d is the Gibbs free energy change of denaturation at various concentrations of Gdn·HCl, $\Delta G_d^{H_2O}$ is that at zero concentration of GdnHCl, and m is a constant related to the susceptibility of the enzyme toward denaturation by the denaturant. The $\Delta G_d^{H_2O}$ values, the midpoint of the denaturation curve ($D_{1/2}$), and the slope (m) are listed in Table 3.

Table 3: Free Energy of Gdn·HCl-Induced Denaturation[a]

enzymes	$\Delta G_d^{H_2O}$ (kcal/mol)	$D_{1/2}$ (M)	m [kcal/(mol·M)]
WT	9.5	6.9	1.48
L2A	8.7 (−0.8)	6.7	1.33
L2W	8.5 (−1.0)	6.6	1.28
L2R	6.9 (−2.6)	6.2	1.04
W3A	10.9 (+1.4)	6.7	1.63
Q4A	10.5 (+1.0)	6.7	1.56
Q4E	8.4 (−1.1)	6.5	1.29
Q4N	8.2 (−1.3)	6.5	1.27
Q4K	9.5	6.6	1.44
F5A	10.0 (+0.5)	7.0	1.29
F5V	6.5 (−3.0)	6.2	1.03
F5W	6.6 (−2.9)	6.2	1.03
F5Y	11.0 (+1.5)	7.1	1.35
N6A	10.6 (+1.1)	6.7	1.58
N6D	10.0 (+0.5)	6.6	1.51
I9A	4.3 (−5.2)	5.6	0.78
I9S	5.3 (−4.2)	5.7	0.93
I9V	9.6 (+0.1)	7.0	1.50
I9F	7.5 (−2.0)	6.4	0.99
I9Y	6.1 (−3.4)	6.1	1.00

[a] Numbers in parentheses are differences between mutants and WT, i.e., $\Delta\Delta G_d^{H_2O}$. The error limit in $\Delta G_d^{H_2O}$ is estimated to be ±0.5 kcal/mol.

The data show that the conformational stability is not appreciably perturbed in the mutants of Leu-2, Trp-3, Gln-4, and Asn-6. In fact, the conformational stabilities of three alanine mutants, W3A, Q4A, and N6A, are enhanced by 1.0−1.4 kcal/mol compared to WT. On the other hand, the conformational stabilities of the mutants of Phe-5 and Ile-9, whose side chains are buried in the hydrophobic channel, are substantially decreased. Substitution of Ile-9 with either Ala or Ser resulted in a 4−5 kcal/mol loss of conformational stability. Replacement of Ile-9 by either Phe or Tyr did not damage the $\Delta G_d^{H_2O}$ of PLA2 as significantly as I9A or I9S but did cause a loss of 2−3 kcal/mol. The most conservative mutant I9V keeps its conformation stability intact. For the Phe-5 mutants, F5W and F5V showed a loss of about 3 kcal/mol of the $\Delta G_d^{H_2O}$ value, while replacement of Phe-5 by Tyr or Ala resulted in an intact conformational stability.

Proton NMR. In accordance with the previous work in our laboratory and other's (Dupureur et al., 1992a,b; Li et al., 1994; Fisher et al., 1989), the NMR analyses of bovine PLA2 were performed at 1.5 mM and pH* 4−5. At higher concentration and/or neutral pH the resonances are less well resolved possibly due to microaggregation. Although the enzyme has little activity at acidic pH, it is not denatured and can be reversibly converted to neutral pH.

(A) Leu-2, Trp-3, Gln-4, and Asn-6 Mutants. In consistence with the results of kinetics and conformational stability, the mutants of surface residues Leu-2, Trp-3, Gln-4, and Asn-6 display only minor perturbations in proton NMR properties (with the exception of the highly hydrophilic mutant L2R; Q4K was not analyzed). Figure 4 shows the NOESY spectra of the aromatic−aromatic and aromatic−aliphatic regions for WT and some of the mutants, W3A, Q4A, and N6D. Qualitatively, the NOESY spectrum of Q4A again shows the greatest perturbation among the three mutants. This is expected since the side chain of Gln-4 is part of the H-bonding network as shown in Figure 1. However, most of the NOESY cross peaks are still observ-

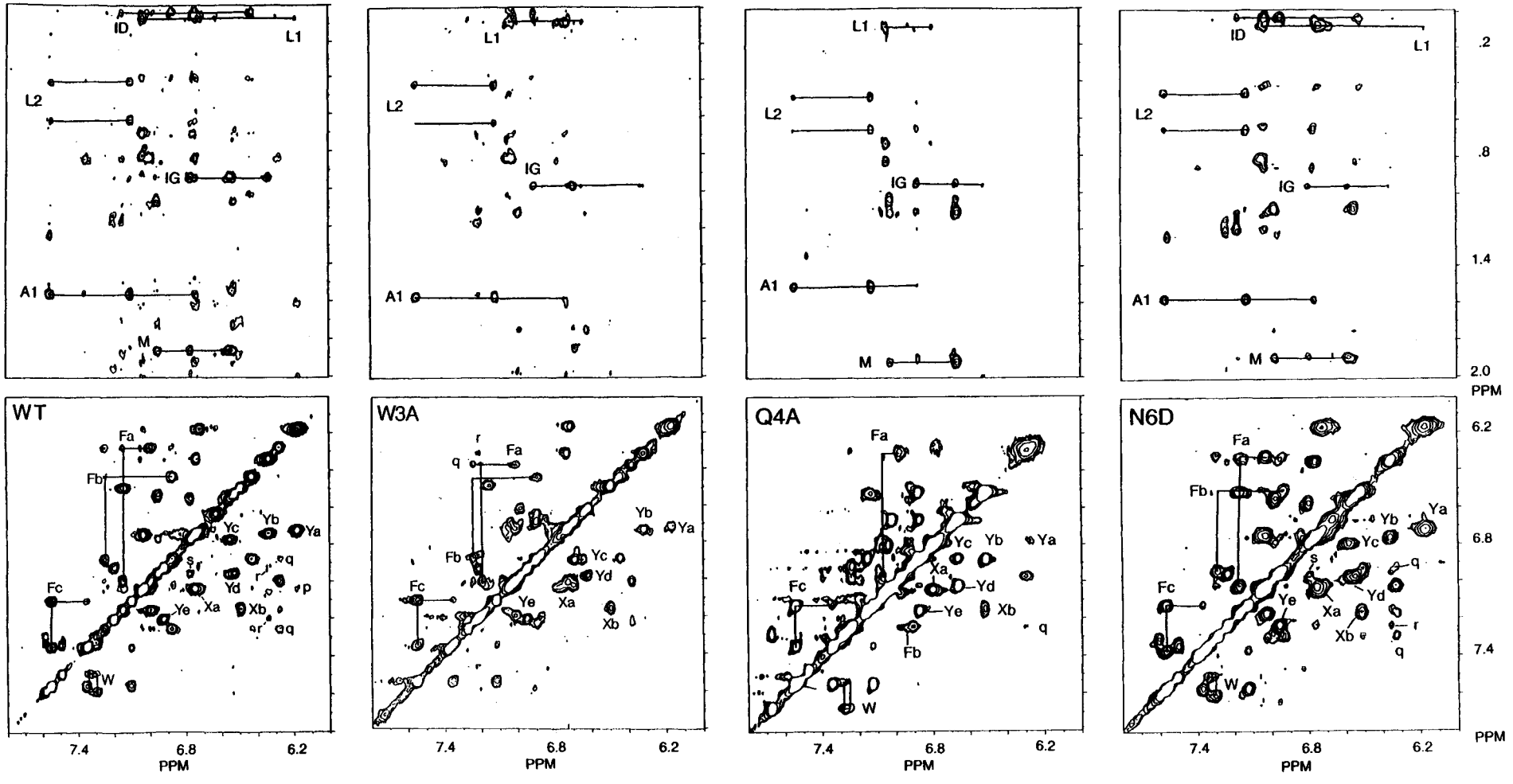

FIGURE 4: Phase-sensitive NOESY spectra of WT, W3A, Q4A, and N6D in D_2O at 500 MHz. The WT spectrum was reproduced from Dupureur et al. (1992a). Sample conditions: 1.5 mM PLA2, 300 mM NaCl, and 50 mM $CaCl_2$, pH* 4.0, at 37 °C. The mixing time was 200 ms. A 4096 × 512 matrix in the time domain was recorded and zero-filled to a 4096 × 2048 matrix prior to multiplication by a Gaussian function (LB −3, GB 0.1). The possible identities of the spin systems are indicated in the first two columns of Table 4. The NOE cross peaks p, q, r, and s arise from Ya/Xa, Fa/Fb, Yb/Ye, and Yc/Yd, respectively.

Table 4: Chemical Shifts of the Assigned Residues for WT and Mutants[a]

spin system[b]	possible assignments	WT			L2W			W3A			Q4A			N6D		
Fa	(F5)	6.28	7.00	7.15		6.33	6.91	6.38	7.02	7.20	6.29	6.98	7.06	6.34	7.03	7.17
Fb	F106	6.43	6.88	7.26	6.45	6.92	7.40	6.45	6.88	7.24		6.91	7.25	6.51	6.93	7.29
Fc	F94	7.10	7.35	7.55	7.13	7.38	7.57	7.12	7.38	7.55	7.13	7.35	7.55	7.13	7.37	7.57
Ya	Y111	6.18	6.72		6.24	6.78		6.16	6.72		6.27	6.79		6.17	6.72	
Yb	Y52	6.34	6.74		6.38	6.80		6.31	6.73		6.51	6.89		6.38	6.76	
Yc	Y73	6.55	6.78		6.53	6.74		6.55	6.90		6.66	6.88		6.58	6.80	
Yd	Y75	6.52	6.95		6.54	6.97		6.62	6.99		6.66	7.03		6.55	6.98	
Ye	Y69	6.92	7.20					6.94	7.22		6.87	7.16		6.85	7.24	
W	W3	7.30	7.34	7.48							7.24	7.28	7.54	7.31	7.35	7.52
		7.58									7.68			7.60		
Xa	(F22)	6.75	7.04					6.72	7.02		6.59	7.05		6.74	7.04	
Xb	(Y28)	6.49	7.15					6.49	7.16		6.52	7.15		6.51	7.18	
ID	(I9)	0.05			0.03									0.03		
L1	(L41)	0.07			0.08			0.09			0.11			0.07		
L2	L58	0.63	0.44		0.64	0.45		0.64	0.42		0.66	0.49		0.65	0.46	
IG	I95	0.94			0.97			0.97			0.94			0.97		
A1	(A55)	1.56			1.58			1.56			1.52			1.58		
M	(M8)	1.86			1.81						1.92			1.90		

[a] The underlined values are resonances which differ by >0.10 ppm between WT and mutant. [b] The designation of spin systems is based on previous work in this laboratory and other laboratories (Dupureur et al., 1992a,b; Fisher et al., 1989). Parentheses indicate tentative assignments.

able even in the spectrum of Q4A. Thus Q4A does not display a large increase in conformational dynamics as in the cases of D99N (Dupureur et al., 1992c), H48N, and H48A (Li & Tsai, 1993).

Semiquantitative comparison can be made from chemical shifts. On the basis of the NOESY and COSY (not shown) spectra, the chemical shifts of most of the aromatic and some of the aliphatic resonances of WT, L2W, W3A, Q4A, and N6D have been assigned and listed in Table 4. There is no resonance which differs by >0.10 ppm between WT and N6D, and only one resonance (underlined) differs by >0.10 ppm between WT and L2W or W3A. Thus it can be concluded that the conformations of L2W, W3A, and N6D are little perturbed from that of WT. The difference between WT and Q4A is more significant: there are five resonances from four residues (Phe-22, Tyr-52, Tyr-73, and Tyr-75) differing from the corresponding resonances of WT by >0.10 ppm. However, the side chains of two of the four residues (Tyr-52 and Tyr-73) are part of the H-bonding network, and the side chain of Tyr-75 participates directly in an edge-to-face aromatic−aromatic interaction with the side chain of Tyr-73. Furthermore, most of the interresidue NOE cross peaks in the NOESY spectrum of Q4A were observed and identified. These results suggest that the global conformation of the enzyme has not changed; the observed perturbation in the NMR property is caused primarily by small changes in local interactions.

(B) Phe-5 Mutants. As shown by the 1D spectra (Figure 5) and 2D NOESY spectra (Figure 6), the conformations of the nonaromatic mutants F5A and F5V are perturbed to a greater extent than the aromatic mutants F5Y and F5W. This can be explained by the fact that the aromatic ring of Phe-5 forms an edge-to-face pair with the aromatic ring of Phe-106. The edge-to-face aromatic ring pair has been demonstrated to be energetically preferred and could be important for enzyme conformation (Burley & Petsko, 1988; Serrano et al., 1991).

(C) Ile-9 Mutants. Figure 7 shows the 1D proton NMR spectra of WT, I9V, I9A, I9F, and I9Y. With the exception of the conservative I9V mutant, the resonance positions are substantially different, the signals are broader, and the nonexchangeable NH protons (7.7−9.5 ppm) are fewer in

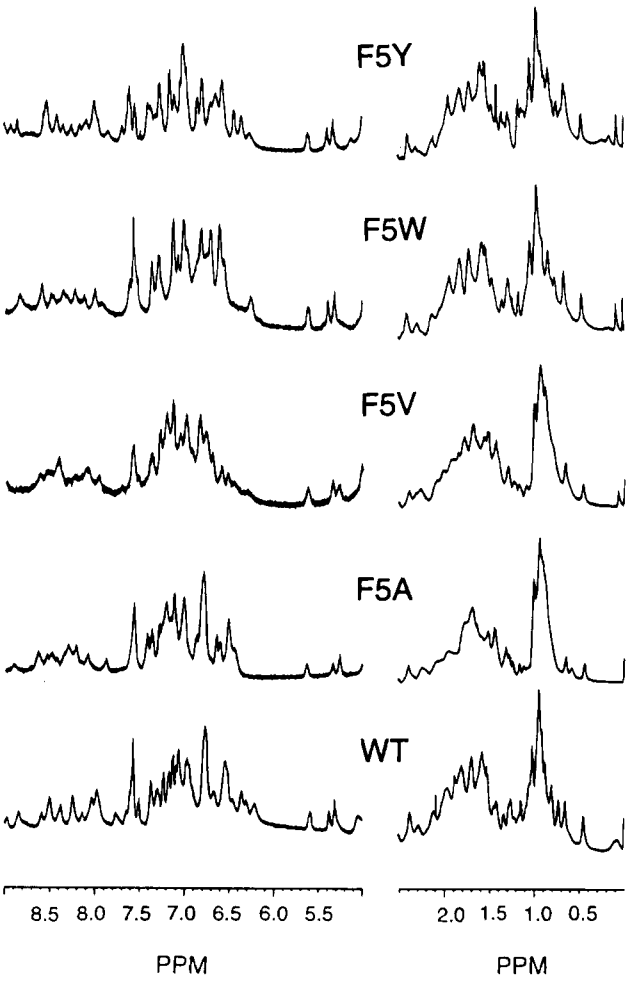

FIGURE 5: One-dimensional proton NMR spectra of WT, F5A, F5V, F5Y, and F5W. Sample conditions are the same as Figure 4. Sample conditions were described in Materials and Methods. The FID from 200 scans were processed with Gaussian multiplication (line broadening −5, Gaussian broadening 0.1) prior to Fourier transformation.

the mutants. The 2D NOESY spectra, as shown in Figure 8, indicate that I9A, I9F, and I9Y have lost many of the NOESY cross peaks (the spectrum of I9V, which is not shown in Figure 8, is very similiar to that of WT). These properties suggest that the conformational dynamics of these

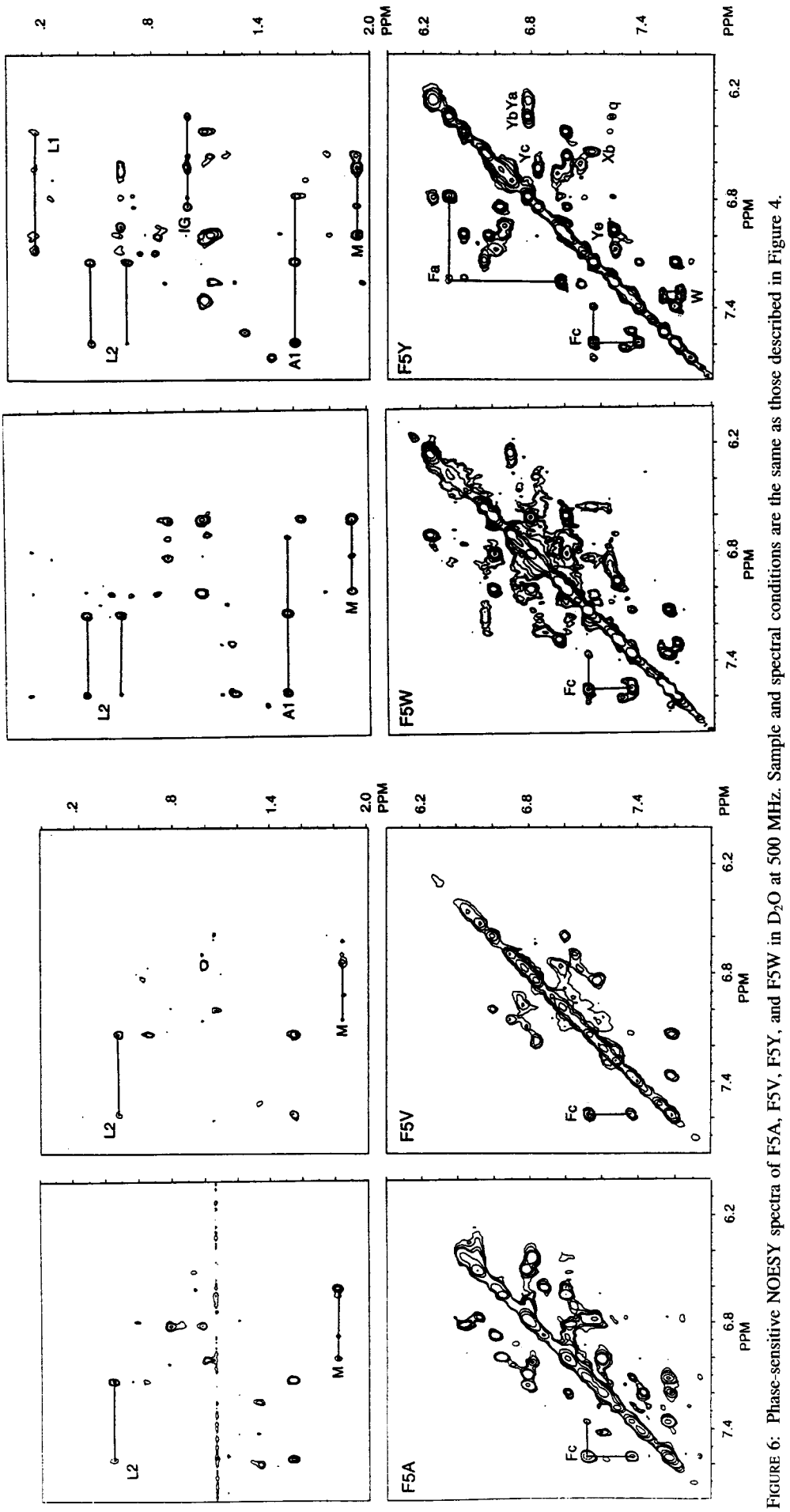

FIGURE 6: Phase-sensitive NOESY spectra of F5A, F5V, F5Y, and F5W in D_2O at 500 MHz. Sample and spectral conditions are the same as those described in Figure 4.

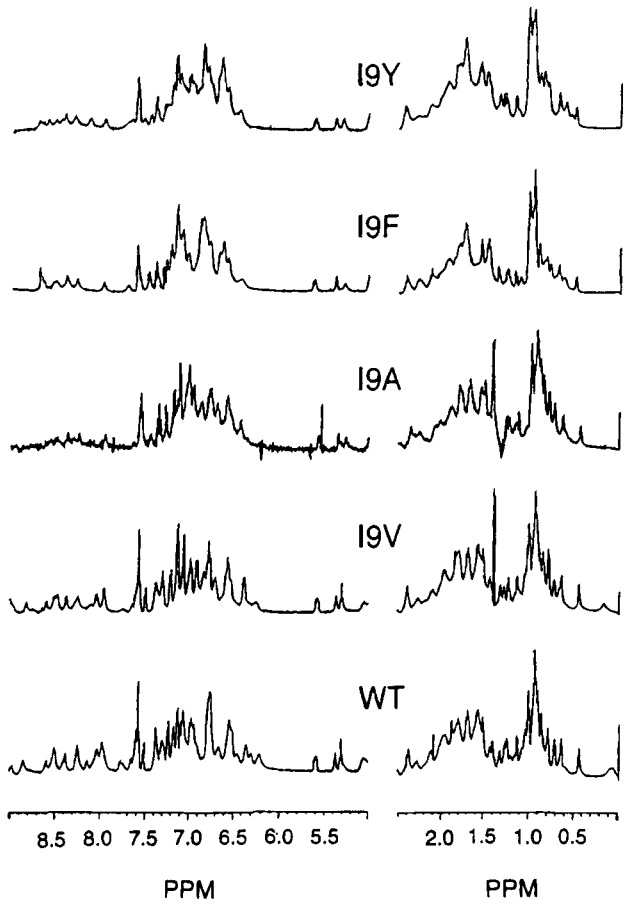

FIGURE 7: One-dimensional proton NMR spectra of WT, I9V, I9A, I9F, and I9Y. Sample and spectral conditions are the same as in Figure 5.

three mutants increase substantially, though not as serious as has been observed previously for D99N and Y73S (Dupureur et al., 1992c) and H48N and H48A (Li & Tsai, 1993). Also in agreement with the previous mutants, the CD spectra of I9A, I9F, and I9Y are only perturbed to a small extent, suggesting that the changes in NMR reflect more of the dynamics than the global conformation.

The 1D and 2D NOESY spectra of the double mutant F5V/I9F (not shown) are very similar to the corresponding spectra of I9F. In conjunction with the result of catalytic activity, it is concluded that the attempt to construct a wild-type-like mutant by replacing Phe-5 with a nonaromatic hydrophobic residue and Ile-9 with an aromatic residue is unsuccessful.

X-ray Crystallography. The rms difference between the mutant Q4E and the WT for all the C_α atoms is only 0.15 Å, implying a remarkable conservation of the overall structure. In fact, none of the C_α atoms differ significantly between the two structures, and all deviations are within 2 times the r.m.s difference between the mutant and the WT. The rms difference between Q4E and the WT for all atoms of the catalytic site is remarkably low (0.07 Å), indicating that the catalytic triad has remained intact. The hydrogen-bonding network which indirectly links Asp-99 to Gln-4 in the WT through a hydrogen bond network involving Ala-1 and a structural water (shown in Figure 1) also remains unaffected in the mutant.

On the other hand, significant differences are observed in the vicinity of the mutation site. The rms deviation for all atoms of residue 4 and those of the neighboring residues (Ala-1, Asn-71, Asn-72, and Tyr-73) is 0.71 Å. The hydrogen-bonding pattern around residue 4 in the WT, Q4E, and an overlay of the two is shown in Figure 9. Most noticeably, there is a water molecule, close to Glu-4, in the mutant which is not present in the WT. The hydrogen bond between the ammonium group of Ala-1 and the side-chain carbonyl group of Gln-4 of the WT remains unaffected in the mutant but the two hydrogen bonds from the NH_2 group of Gln-4 to the backbone carbonyl groups of Asn-71 and Tyr-73 are lost in the mutant. Instead, the $O_{\epsilon 2}$ of Glu-4 in the mutant is hydrogen bonded to the water molecule. Thus, the mutation of the neutral glutamine to the charged glutamate has, in effect, resulted in replacing the two hydrogen bond donor interactions at residue 4 by a hydrogen bond acceptor interaction. Besides, there is a significant change in the side-chain conformation of residue 4 (the χ_2, χ_3 values for the WT are 108° and 130°, respectively, as against 69° and −143° for the Q4E mutant). In the WT, the distances (Gln-4)$N_{\epsilon 2}\cdots$O=C(Tyr-73) and (Gln-4)-$N_{\epsilon 2}\cdots$O=C(Asn-71) are 3.2 and 2.9 Å, respectively. The corresponding distances in the mutant, (Glu-4)$O_{\epsilon 2}\cdots$O=C-(Tyr-73) and (Glu-4)$O_{\epsilon 2}\cdots$O=C(Asn-71), are 5.5 and 4.8 Å, respectively. There is, however, no void in this region in Q4E, which is probably due to the presence of the new water molecule.

From the X-ray structure of the Q4E mutant it is clear that the overall structure, the catalytic triad, and the link between residue 4 and Asp-99 via hydrogen bonding through Ala-1 and the structural water remain the same as in the WT. Only significant structural differences between the WT and mutant involve the side chain of residue 4. These results are in agreement with the proton NMR and kinetic studies of the Q4E mutant.

DISCUSSION

Summary of Results. This paper describes detailed structural and functional characterization of 20 site-specific mutants of the N-terminal residue, Leu-2, Trp-3, Gln-4, Phe-5, Asn-6, and Ile-9 of phospholipase A_2 from bovine pancreas. Overall, the perturbations in the structural and functional properties are minimal or modest for the mutants of surface residues Leu-2, Trp-3, Gln-4, and Asn-6 but are significant for those of Phe-5 and Ile-9, whose side chains are part of the interior wall of the hydrophobic channel. In addition, the E to E* step on $DC_{14}PM$ vesicles has been perturbed for W3A. The implications of the structural and kinetic results on the mechanism of interfacial catalysis are discussed as follows:

Hydrophobic Channel Residues: Leu-2, Phe-5, and Ile-9. The crystal structure of the complex of snake venom PLA2 and a transition-state analog L-1-O-octyl-2-(heptylphosphonyl)-*sn*-glycero-3-phosphoethanolamine (White et al., 1990; Scott et al., 1990) indicates that the side chains of the three hydrophobic channel residues (Leu-2, Phe-5, and Ile-9) could contribute to substrate binding or orientation, presumably at the transition state, by providing their hydrophobic surface to contact the acyl chain of the substrate. The X-ray crystal structure of porcine pancreatic PLA2 complexed with the inhibitor 2-(dodecanoylamino)-1-hexanol phosphoglycol also shows that Ile-9 is located close to the *sn*-2 acyl chain, with its δ-methyl located only 3.60 Å away from C9 of the *sn*-2 acyl chain of the inhibitor (Thunnissen et al., 1990). Evidence for direct interaction between Ile-9 and Phe-5 side chains and the transition-state analogs has

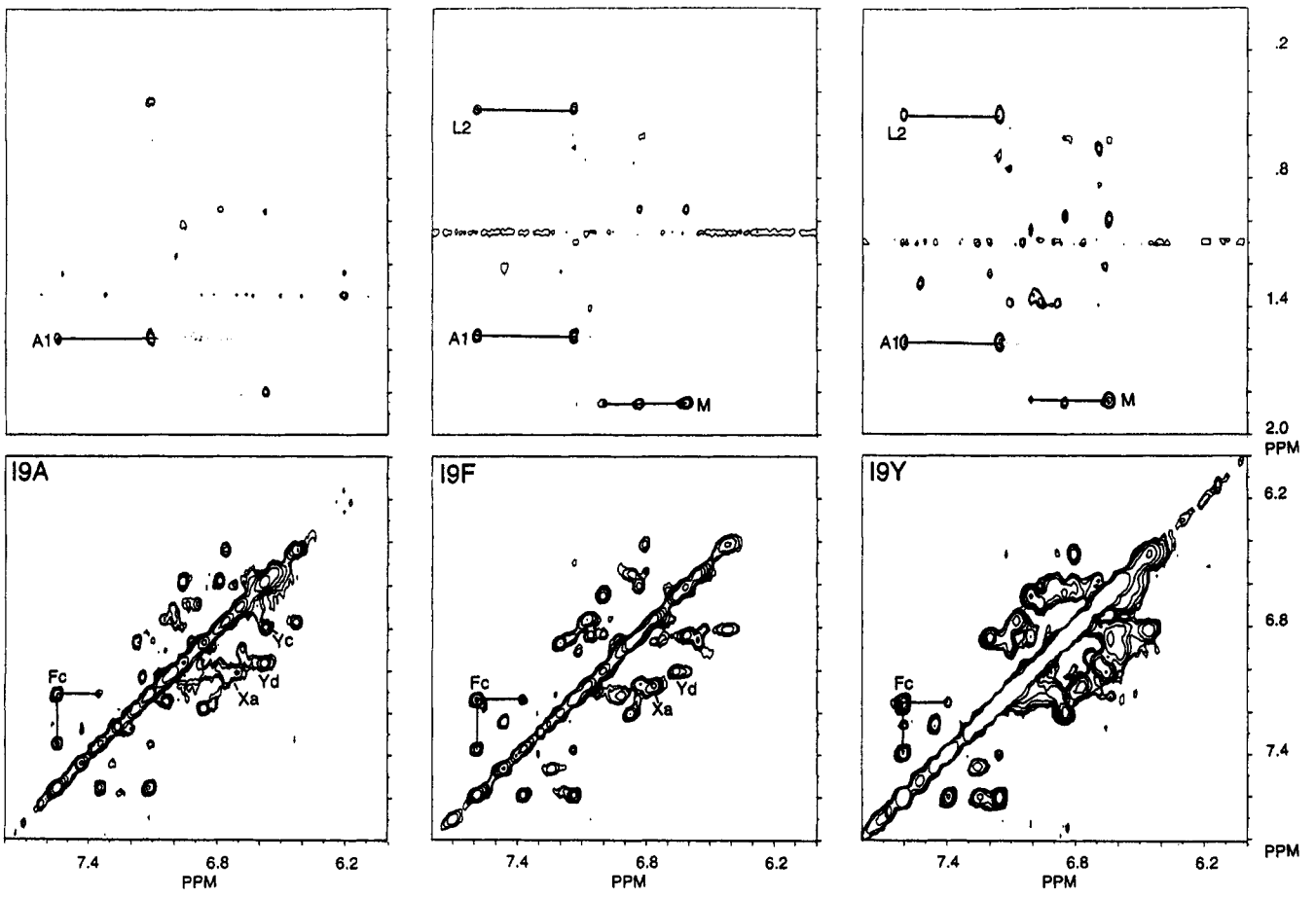

FIGURE 8: Phase-sensitive NOESY spectra of I9A, I9F, and I9Y in D_2O at 500 MHz. Sample and spectral conditions are the same as those described in Figure 4.

also been provided by the inhibitor–protein NOEs of porcine pancreatic PLA2 bound to a micellar lipid–water interface of different substrate-derived competitive inhibitors (Dekker et al., 1991; Peters et al., 1992). In their studies, large chemical shift changes for Ile-9 and Phe-5 were observed when the inhibitors bound to the active site. The δ-methyl group of Ile-9 was clearly shown to interact at position C9 or C10 of the competitive inhibitors, while a strong intermolecular NOE from the aromatic protons of Phe-5 can be clearly assigned to one of the methylene protons of the *sn*-2 chain of the inhibitor. The NMR analyses, however, did not identify direct contact of the Leu-2 side chain with the inhibitor.

As discussed in Results, most of the Phe-5 and Ile-9 mutants show varying degrees of conformational perturbations. Thus the changes in kinetic parameters should be considered only as the possible "maximal effect" for the mutation of the particular residue; it can be contributed by *both* structural and functional effects. On the other hand, since at least one mutant at each position has been shown to display little perturbation in proton NMR properties or in conformational stability, one can be certain about the functional roles of these mutants.

The results from this study suggest that a hydrophobic side chain of an appropriate size at position Ile-9 and Phe-5 is important for enzyme catalysis. Removal of the hydrophobic bulk or introduction of hydrophilicity led to decreases of up to 200-fold in the $k_{cat,app}$ toward DC_8PC micelles and the v_0 toward $DC_{14}PM$ vesicles. The changes appear to be the greatest when the steric bulk of the side chain increases. Detailed scooting mode kinetic analysis at the interface led to the conclusion that the specific step of change lies in k_{cat}, the chemical step; i.e., the hydrophobic function of these residues appears to come into play only at the transition state. The K_S* and K_M* values of the mutants are the same as or somewhat lower than those of WT. These results clearly provide a functional basis for the observation from the crystal structures. Similar kinetic results have been observed for mutants of Phe-22 and Phe-106 (Dupureur et al., 1992b), which are located near Phe-5. Thus these residues could play similar functional roles.

The kinetic data for Leu-2 mutants show an interesting trend: the L2W mutant is unperturbed in rates of hydrolyses of DC_8PC or DC_8PM micelles but is significantly perturbed in the v_0 of $DC_{14}PM$ vesicles, and the L2R mutant shows 120–450-fold decreases in the rates of hydrolyses of DC_8-PC or DC_8PM micelles but an even greater decrease (23 600-fold) in the v_0 of $DC_{14}PM$ vesicles. These are contrary to most, if not all, of the mutants studied previously, for which the degree of change in v_0 is usually comparable to or smaller than the degree of change in $k_{cat,app}$. This can be explained by the fact that the "hydrophobic tail" of $DC_{14}PM$ is substantially longer than that of DC_8PC or DC_8PM. According to the crystal structure of the porcine pancreatic PLA2–inhibitor complex (Thunnissen et al., 1990), the side chain C_γ of Leu-2 is 3.65 Å away from the C_{12} of the *sn*-2 chain of the inhibitor 2-(dodecanoylamino)-1-hexanol phosphoglycol.

The most conservative mutant I9V behaved like a wild-type enzyme, and only slight changes in $k_{cat,app}$ and $K_{m,app}$ were observed. The kinetic results suggest that the δ-methyl group of the Ile residue is not essential for the catalytic

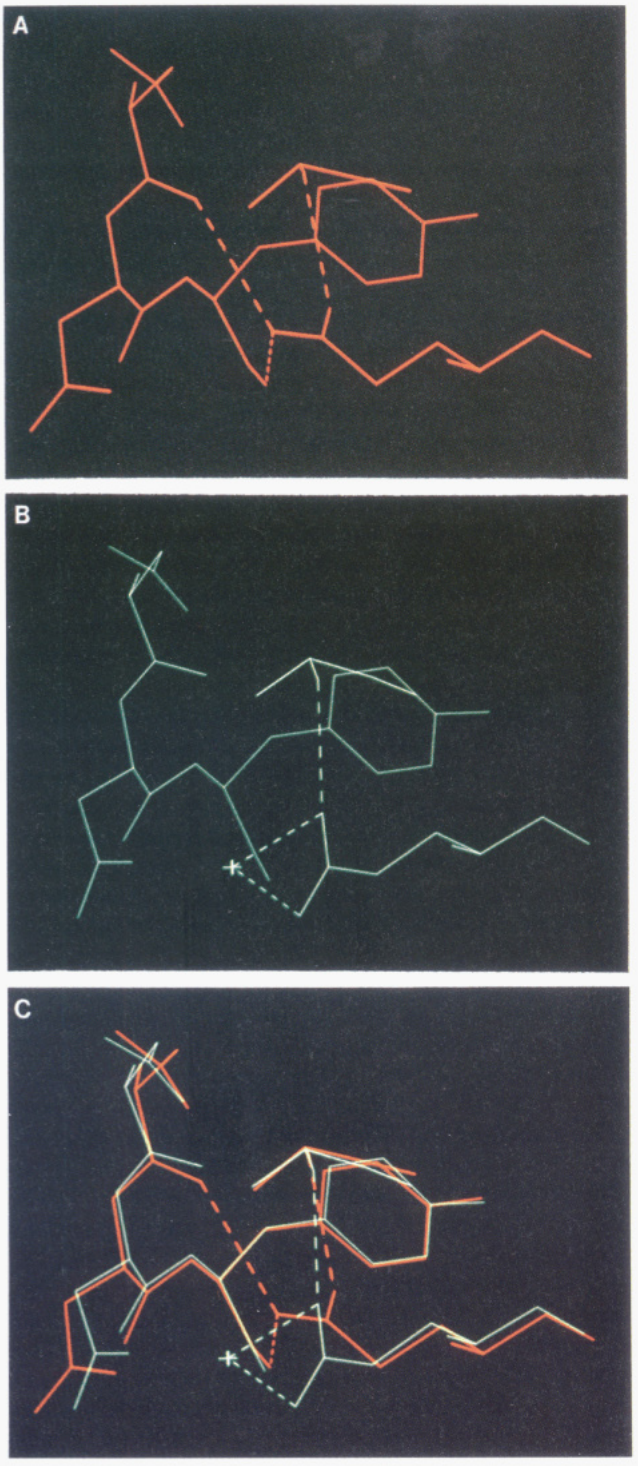

FIGURE 9: Hydrogen-bonding interactions involving the side chain of residue 4 in (A) the WT, (B) the mutant Q4E, and (C) the overlay of (A) and (B), as revealed by the crystal structures.

function, and the results of structural analyses suggest that the conformation of this mutant is largely unperturbed relative to WT. These findings are interesting since Ile is the absolutely conserved residue at this position; there is no known natural variant with a Val substitution at this position. In addition, a previous NMR study concluded that the δ-methyl group of Ile-9 is in contact with the *sn*-2 acyl chain of a competitive inhibitor (Peters et al., 1992).

H-Bonding Network Residue: Gln-4. Gln-4 is a highly conserved residue at the N-terminus and is part of the hydrogen-bonding network as shown in Figure 1. However, our results show that the kinetic parameters of Q4E and Q4N are little perturbed relative to the WT enzyme. This can be explained by the ability of the side chains of Glu and Asn to form a hydrogen bond. In fact, Gln-4 is substituted by Glu or Asn in a few natural variants of PLA2 (Davidson & Dennis, 1990; Heinrikson, 1991). The crystal structure of Q4E confirms that the hydrogen bonding between the side-chain carbonyl oxygen and the amino group of Ala-1 is preserved in Q4E (Figure 9).

The mutant Q4A displays a 2-fold decrease in $k_{cat,app}$ and a 13-fold increase in $K_{m,app}$ toward DC_8PC micelles. Such changes are modest at best, and the changes could be attributed to 3−4-fold increases in K_M* and K_S* in the scooting mode assay using $DC_{14}PM$ vesicles. The E to E* step appears not appreciably perturbed. The results of Q4A suggest that the hydrogen bond between the side chain of Gln-4 and the N-terminal ammonium group is not important for the catalysis. This contradicts an earlier report that substitution of Gln-4 by norleucine semisynthetically resulted in a total loss of affinity for micelles of *cis*-octadecenylphosphocholine because of disruption of the hydrogen-bonding network (van Scharrenburg et al., 1982). The discrepancy could be caused by the fact that norleucine is substantially bulkier than alanine and that the lysine side chains of the semisynthetic mutant are also ϵ-amidinated. In any case, our result has been corroborated by several recent findings from our laboratories: Disruption of the H-bonding network by deletion of the N-terminal alanine residue led to only small perturbation in kinetic parameters (Maliwal et al., 1994), and substitution of either or both tyrosine groups (52 and 73) with phenylalanine (Dupureur et al., 1992a) resulted in little or no perturbations. Most interestingly, we have found that the D99N mutant still retains 0.5−8% of activity (Dupureur et al., 1992c) despite the fact that the structural water at the center of the hydrogen-bonding network is missing in its crystal structure (Kumar et al., 1994). In both the D99N mutant (Kumar et al., 1994) and the Y52F/Y73F double mutant (Sekharudu et al., 1992), the missing hydrogen bonds were partially compensated for by increased hydrophobic interactions. It remains to be established, presumably by X-ray crystallography, whether this is also the case for the des-1 and the Q4A mutants.

The proton NMR property of Q4A is noticeably perturbed relative to that of WT. However, the result of detailed analyses indicates that the perturbation occurs primarily in two residues (Tyr-52 and Tyr-73) which are connected to Gln-4 through the H-bonding network and another residue (Tyr-75) which interacts directly with Tyr-73. The dramatic increase in conformational dynamics observed for D99N (Dupureur et al., 1992c), H48N, and H48A (Li & Tsai, 1993) is not seen in Q4A. Although these mutants share a common feature that the H-bonding network has been perturbed, Q4A differs from the rest in that the hydrogen bond in question connects two residues (Gln-4 and Ala-1) within the same N-terminal helical segment. For the other three mutants, the two residues contributing to the hydrogen bond (Asp-99 and His-48) are located in two separate helices; thus the hydrogen bond between them could be structurally important.

"Interfacial Site" Residues: Trp-3 and Asn-6. It has been generally accepted in "the field that the interfacial binding site of PLA2 includes the N-terminal region. Fluorescence studies have clearly established that Trp-3 is on the interfacial binding surface and may be involved in the binding to aggregated substrate (Jain & Vaz, 1987; Ludescher et al., 1988). However, the kinetic data of N6A and N6D toward DC_8PC micelles and $DC_{14}PM$ vesicles are not altered by more than a factor of 3. The kinetic data of W3A are

perturbed only modestly toward DC_8PC micelles and DC_{14}-PM vesicles; detailed analyses indicate that the perturbation lies in both the E to E* step and the E* to E*S step. Earlier site-directed mutagenesis studies on the third residue, Leu-31 (of porcine pancreatic PLA2), also indicated only modest changes toward DC_8PC micelles (Kuipers et al., 1990). The $k_{cat,app}$ of L31A toward DC_8PC micelles decreases by 30-fold, while the $K_{m,app}$ is unchanged; the change in $k_{cat,app}$ should be considered as an upper limit only since the structure of the mutant was not characterized in the work by Kuipers et al. (1990).

The lack of effects of the N6 mutants and the modest effects of the W3 and L31 mutants support the theory that the interfacial binding site for PLA2 involves a large number of residues (Dijkstra et al., 1981b; Ramirez & Jain, 1991). Thus a change in one of them would have only an incremental change in the underlying kinetic parameters, rather than an all or none effect. Furthermore, these observations call in question any theory that postulates a unique conformation for the E, E*, and E*L forms of the enzyme because all such states are formed even when the hydrogen bonding network has been partially disrupted as discussed in the previous section. As an alternative one of us has proposed that PLA2 (at least its N-terminus) exists in an ensemble of conformations which adapt to a range of interfaces formed from a variety of phospholipids and amphiphiles (Jain & Maliwal, 1993; Maliwal et al., 1994). Further studies will be required to delineate the role of the N-terminal residues in the nature of interfacial binding.

REFERENCES

Atkins, G. L., & Nimmo, I. A. (1975) *Biochem. J. 149*, 775−779.

Berg, O. G., Yu, B.-Z., Rogers, J., & Jain, M. K. (1991) *Biochemistry 30*, 7283−7297.

Brünger, A. T. (1992) *X-PLOR Manual*, Yale University, New Haven, CT.

Burley, S. K., & Petsko, G. A. (1988) *Adv. Protein Chem. 39*, 125−189.

Carson, M. (1991) *Ribbons 2.0 Manual*, Univesity of Alabama, Birmingham.

Davidson, F. F., & Dennis, E. A. (1990) *J. Mol. Evol. 31*, 228−238.

Dekker, N., Peters, A. R., Slotboom, A. J., Boelens, R., Kaptein, R., Dijkman, R., & de Haas, G. H. (1991) *Eur. J. Biochem. 199*, 601−607.

Deng, T., Noel, J. P., & Tsai, M.-D. (1990) *Gene 93*, 229−234.

Dijkstra, B. W., Kalk, K. H., Hol, W. G. J., & Drenth, J. (1981a) *J. Mol. Biol. 147*, 97−123.

Dijkstra, B. W., Drenth, J., & Kalk, K. H. (1981b) *Nature 289*, 604−606.

Dijkstra, B. W., Renetseder, R., Kalk, K. H., & Drenth, J. (1983) *J. Mol. Biol. 168*, 163−179.

Dijkstra, B. W., Kalk, K. H., Drenth, J., de Haas, G. H., Egmond, M. R., & Slotboom, A. J. (1984) *Biochemistry 23*, 2759−2766.

Dupureur, C. M., Deng, T., Kwak, J.-G., Noel, J. P., & Tsai, M.-D. (1990) *J. Am. Chem. Soc. 112*, 7074−7076.

Dupureur, C. M., Yu, B.-Z., Jain, M. K., Noel, J. P., Deng, T., Li, Y., Byeon, I.-J. L., & Tsai, M.-D. (1992a) *Biochemistry 31*, 6402−6413.

Dupureur, C. M., Yu, B.-Z., Mamone, J. A., Jain, M. K., & Tsai, M.-D. (1992b) *Biochemistry 31*, 10576−10583.

Dupureur, C. M., Li, Y., & Tsai, M.-D. (1992c) *J. Am. Chem. Soc. 114*, 2748−2749.

Fisher, J., Primrose, W. U., Roberts, G. C. K., Dekker, N., Boelens, R., Kaptein, R., & Slotboom, A. J. (1989) *Biochemistry 28*, 5939−5946.

Ghomashchi, F., Yu, B.-Z., Berg, O., Jain, M. K., & Gelb, M. H. (1991) *Biochemistry 30*, 7318−7329.

Heinrikson, R. L. (1991) *Methods Enzymol. 197*, 201−214.

Howard, A. J. (1990) *The XENGEN System, Version 2.0*, Genex Corp., Gaithersburg, MD.

Jain, M. K., & Vaz, W. L. C. (1987) *Biochim. Biophys. Acta 906*, 1−8.

Jain, M. K., & Berg, O. G. (1989) *Biochim. Biophys. Acta 1002*, 127−156.

Jain, M. K., & Rogers, J. (1989) *Biochim. Biophys. Acta 1003*, 91−97.

Jain, M. K., & Gelb, M. H. (1991) *Methods Enzymol. 197*, 112−125.

Jain, M. K., & Maliwal B. P. (1993) *Biochemistry 32*, 11838−11846.

Jain, M. K., Rogers, J., Jahagirdar, D. V., Marecek, J. F., & Ramirez, F. (1986) *Biochim. Biophys. Acta 860*, 435−447.

Jain, M. K., Yu, B.-Z., Rogers, J., Ranadive, G. N., & Berg, O. G. (1991a) *Biochemistry 30*, 7306−7317.

Jain, M. K., Rogers, J., Berg, O. G., & Gelb, M. H. (1991b) *Biochemistry 30*, 7340−7348.

Jain, M. K., Tao, W., Rogers, J., Arenson, C., Eibl, H., & Yu, B.-Z. (1991c) *Biochemistry 30*, 10256−10268.

Jain, M. K., Yu, B.-Z., & Berg, O. G. (1993) *Biochemistry 32*, 11319−11329.

Jain, M. K., Gelb, M. H., Rogers, J., Berg, O. G., & Gelb, M. H. (1995) *Methods Enzymol. 249*, 567−614.

Jones, T. A. (1985) *Methods Enzymol. 115*, 157−171.

Kuipers, O. P., Kerver, J., Van Meersbergen, J., Vis, R., Dijkman, R. M., Verheij, H. M., & de Hass, G. H. (1990) *Protein Eng. 3*, 599−603.

Kumar, A., Sekharaudu, Y. C., Dupureur, C. M., Zhu, H., Tsai, M.-D., & Sundaralingam, M. (1994) *Protein Sci. 3*, 2082−2088.

Li, Y., & Tsai, M.-D. (1993) *J. Am. Chem. Soc. 115*, 8523−8526.

Li, Y., Yu, B.-Z., Zhu, H., Jain, M. K., & Tsai, M.-D. (1994) *Biochemistry 33*, 14724−14732.

Ludescher, R. D., Johnson, I. D., Volwerk, J. J., de Hass, G. H., Jost, P. C., & Hudson, B. S. (1988) *Biochemistry 27*, 6618−6628.

Maliwal, B. P., Yu, B.-Z., Szmacinksi, H., Squier, T., Binsbergen, J. V., Slotboom, A. J., & Jain, M. K. (1994) *Biochemistry 33*, 4509−4516.

Noel, J. P., Bingman, C., Deng, T., Dupureur, C. M., Hamilton, K. J., Jiang, R.-T., Kwak, J.-G., Sekharudu, C., Sundaralingam, M., & Tsai, M.-D. (1991) *Biochemistry 30*, 11801−11811.

Nozaki, Y. (1972) *Methods Enzymol. 26*, 43−50.

Pace, C. N. (1986) *Methods Enzymol. 131*, 266−280.

Peters, A. R., Dekker, N., van den Berg, L., Boelens, R., Slotboom, A. J., de Haas, G. H., & Kaptein, R. (1992) *Biochimie 74*, 859−866.

Ramirez, F., & Jain, M. K. (1991) *Proteins 9*, 229−239.

Sanger, F., Niklen, S., & Coulson, A. R. (1977) *Proc. Natl. Acad. Sci. U.S.A. 74*, 5463−5467.

Scott, D. L., White, S. P., Otwinowski, Z., Yuan, W., Gelb, M. H., & Sigler, P. B. (1990) *Science 250*, 1541−1546.

Sekharudu, C., Ramakrishnan, B., Huang, B., Jiang, R.-T., Dupureur, C. M., Tsai, M. D., & Sundaralingam, M. (1992) *Protein Sci. 1*, 1585−1594.

Serrano, L., Bycroft, M., & Fersht, A. R. (1991) *J. Mol. Biol. 218*, 465−475.

Thunnissen, M. M. G. M., Ab, E., Kalk, K. H., Drenth, J., Dijkstra, B. W., Kuipers, O. P., Dijkman, R., de Hass, G. H., & Verheij, H. M. (1990) *Nature 347*, 689−691.

Tzeng, M.-C., Yen, C.-H., Hseu, M.-J., Dupureur, C. M., & Tsai, M.-D. (1995) *J. Biol. Chem. 270*, 2120−2123.

van den Bergh, C. J., Slotboom, A. J., Verheij, H. M., & de Haas, G. H. (1989) *J. Cell. Biochem.* 39, 379−390.

van Scharrenburg, G. J. M., Puijk, W. C., Egmond, M. R., van der Schaft, P. H., de Hass, G. H., & Slotboom, A. J. (1982) *Biochemistry 21*, 1345−1352.

van Scharrenburg, G. J. M., Puijk, W. C., Seeger, P. R., de Hass, G. H., & Slotboom, A. J. (1984a) *Biochemistry 23*, 1256−1263.

van Scharrenburg, G. J. M., Jansen, E. H. J. M., Egmond, M. R., de Hass, G. H., & Slotboom, A. J. (1984b) *Biochemistry 23*, 6285−6294.

White, S. P., Scott, D. L., Otwinowski, Z., Gelb, M. H., & Sigler, P. (1990) *Science 250*, 1560−1563.

Yu, B.-Z., Berg, D. G., & Jain, M. K. (1993) *Biochemistry 32*, 6485−6492.

BI9426219